Thermal denaturation of double-stranded DNA: Effect of base stacking

Mohammad Kohandel
Department of Applied Mathematics, University of Waterloo, Waterloo, Ontario N2L 3G1, Canada

Bae-Yeun Ha*
Department of Physics, University of Waterloo, Waterloo, Ontario N2L 3G1, Canada
(Received 16 August 2005; published 11 January 2006)

We study the thermal denaturation of double-stranded DNA, i.e., separation of its two strands upon heating. A simple homo-polymer model is used to account for the effect of base stacking on the thermal stability of DNA. We find that stacking influences the stability in a nontrivial way: It not only enhances the stability but also makes the denaturation transition sharp. While stacking between bound monomers stabilizes DNA as does base pairing, stacking in unbound parts (or loops) rather destabilizes DNA—the overall stability is, however, enhanced by stacking.

DOI: 10.1103/PhysRevE.73.011905 PACS number(s): 87.14.Gg, 05.70.Fh

I. INTRODUCTION

DNA is a double-stranded (ds) chain molecule formed by two separate strands, each consisting of chain segments or monomers [1]. The two strands are wound round each other with base pairing, i.e., the "key and lock" bonding between Watson-Crick pairs. The dsDNA molecule is stabilized by yet another factor: base stacking within each strand [2]. Unlike covalent bonds, these interactions can be disturbed relatively easily by thermal fluctuations or external perturbations (ligand binding or external forces) [3,4]. This allows DNA to undergo various conformational transitions required for its biological functioning.

Local denaturation of dsDNA, i.e., partial opening of base pairs, is an essential physical step prior to DNA replication and transcription: The dsDNA becomes partially denaturated by an enzyme, exposing its bases to other molecules [1]. Also, dsDNA will denaturate if it is heated up or its two opposing ends are pulled apart [1,4]. The capability of DNA to change its stability against denaturation is crucial for a living cell to survive; it is at the heart of the storage and transmission of genetic information [1,4]. Accordingly, the problem of DNA denaturation has been the subject of extensive experimental and theoretical investigation [5–21]. It is not only of practical interest due to its significance in biology but also of fundamental interest: DNA denaturation is regarded as a rare and novel example of one-dimensional phase transitions [7–21]. The transition can easily be monitored experimentally because it results in a large increase in the absorbance of UV light at ~260 nm [5–8]. Artificial DNA molecules consisting of one type of bases along one strand and complimentary based on the other have been shown to exhibit a sharp denaturation transition. On the other hand, the denaturation of natural DNA molecules occurs in multiple steps in a sequence-dependent way [5–8]. This observation has spurred extensive investigation to study the underlying physics of the denaturation transition—its existence and nature [5–21].

The observation of DNA molecules using cryomicroscopy shows that denaturation starts with local opening of denaturation "bubbles" that grow in size with increasing temperature and coalesce into each other (see, for example, Fig. 2 in Ref. [6], Fig. 7 in Ref. [7], Fig. 4 in Ref. [8], or Fig. 8 in Ref. [9]). This will eventually cause separation of the two strands at the denaturation temperature. In this sense, thermal fluctuations are precursors to denaturation, and the study of DNA stability against thermal denaturation is an essential step toward a better understanding of DNA stability. An early model along this line was discussed by Poland and Scheraga (PS) [11] nearly 40 years ago. In the PS model, a DNA molecule is considered as being composed of an alternating array of bound and denaturated states as schematically illustrated in Fig. 1. Since its introduction, the PS model has been used widely in the literature [12–15]. The entropic (and energetic) weights are different for open bubbles and for double stranded states. The number of conformations of a loop of length ℓ varies as s^{ℓ}/ℓ^{c} for large ℓ, where s is a nonuniversal constant. As it turns out, the existence and characteristics of a denaturation transition are dictated by the exponent c, which depends upon spatial dimensions and excluded volume [11–16] (also see below). Excluded-volume interactions

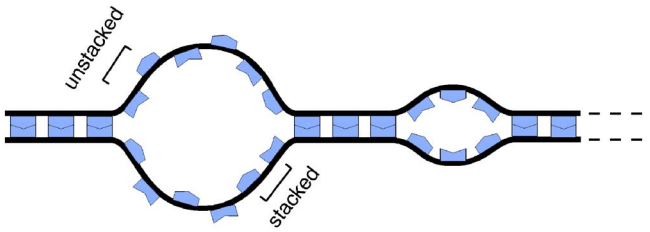

FIG. 1. (Color online) Schematic representation of a locally denaturated DNA molecule. In Poland-Scheraga model, the molecule consists of an alternating array of bound states and loops; if the loops are entropically favored, the bound states are energetically preferred. Accordingly, the thermal stability of DNA is determined by the balance of the two opposing effects: energy and entropy. This consideration is, however, complicated by base stacking in loops—see Sec. II B for details.

*Corresponding author. Email address: byha@uwaterloo.ca

within a loop make the transition sharper (still continuous for $d=2,3$) [16]; when these interactions between loops and the rest of the chain are also included, denatuation becomes a first-order transition [14,15]. Some theoretical approaches include such complexities as DNA sequence heterogeneity [17,18] and helical structures [19,20]. Dynamical aspects of local denaturation can be found in Ref. [22]. Finally, some authors discuss the effect on DNA denaturation of a pulling force acting on the opposing ends of a DNA molecule [23,24].

As briefly mentioned earlier, both base pairing and base stacking stabilize dsDNA against denaturation (see, for example, Ref. [2] and references therein). Electrostatic interactions between bases can also influence the stability but these are not explicitly included here. Base pairing solely cannot account for DNA stability in an aqueous environment, since bases can form hydrogen bonding with surrounding water molecules, meaning that base pairing is relatively weak in water [2]. In a minimalist model, stacking in bounded states can be considered as renormalizing base-pairing energy as done in many theoretical approaches [11–15]. On the other hand, base stacking can occur not only between monomers in bound states but also between those in loops. Recently, the persistence length of single-stranded (ss) DNA has been measured at room temperature as a function of the ambient salt concentration [25]. This measurement suggests that the intrinsic (nonelectrostatic) persistence length ℓ_p ranges from 8 to 13 Å. In this estimate, it was assumed that $b_s=4.3$ Å, where b_s is the inter-base distance of ssDNA. (Note that the value of b_s varies from reference to reference. For example, Smith *et al.* reported $b_s \approx 5.6$ Å [26]; Mills *et al.* find b_s for homogeneous ssDNA to be $b_s \approx 5-7$ Å [27].) Obviously the estimated ℓ_p is much larger than the bare persistence length $\ell_0=b_s/2$. This indicates that base stacking can stiffen ssDNA noticeably. By the same token, bases in loops can be stacked as in ssDNA. It is thus desirable to examine base stacking and base pairing on an equal footing.

The main purpose of this paper is to discuss the effect of base stacking on the DNA stability against thermal denaturation. In particular, we will examine how base stacking influences the DNA stability. To this end, we generalize the grand canonical approach to a PS type model adopted in Refs. [14,15] to incorporate more consistently stacking interactions between two consecutive bases along the same strand. (Note that the approach used in Ref. [13] is essentially the same in spirit as those in Refs. [14,15].) It will thus test a renormalized parameter approach, in which base stacking is considered as enhancing base pairing [11–15]. We use a simple model of stacking introduced in Refs. [28,29]: a two-state model in which two adjacent monomers are either "stacked" or "unstacked." Throughout this paper, we suppress the heterogeneity of bases and assume that all stacked bases gain the same energy: If stacked, i.e., aligned with each other in parallel, they gain stacking energy E_s; otherwise they are free to bend or rotate around each other. The resulting model incorporates base stacking into the commonly used freely-jointed chain (see for example Ref. [30]). Note that this is distinct from the early one [10] that includes "displacement-dependent" stiffness, in which stacking is included when two complimentary bases (in opposing strands) are sufficiently close—in the latter, stacking is not included in loop parts. Using the stacking chain model, we find that the role of stacking is nontrivial: It not only enhances the stability but also makes the denaturation transition *sharp* (even when excluded volume interactions are suppressed). Obviously, stacking between bound monomers tends to stabilize DNA as does base pairing. Interestingly, we find that stacking in unbound parts (or loops) rather destabilizes DNA by making the transition sharper and thus lowering the denaturation temperature. On the other hand, the overall stability of DNA is enhanced by stacking.

The rest of paper is organized as follows. After briefly reviewing PS model in Sec. II A, we introduce our generalized model in Sec. II B, followed by results and discussions in Sec. III.

II. MODELS

A. Grand canonical approach to the PS Model

In Poland-Scheraga (PS) type models, a DNA molecule is considered as an alternating sequence of bound segments and denaturated loops as illustrated in Fig. 1. If loops are favored by the chain entropy, bound states are energetically preferred. The binding energy $E_0<0$ is taken to be the same for all base pairs. With this simplification, the statistical weight for a bound sequence of length ℓ is then given by $w^\ell = \exp(-\ell E_0/k_BT)$, where T is the temperature and k_B is the Boltzmann constant (the monomer size is set to 1). On the other hand, the statistical weight of a denaturated sequence of length ℓ is given by $\Omega(2\ell)=As^\ell/\ell^c$ (for large ℓ), where s is a nonuniversal constant and the exponent c is determined by the properties of the loop configurations (for simplicity, we choose $A=1$). Finally, the precise form of the statistical weight of the denaturated end is not required unless the DNA molecule is fully denaturated (see Ref. [15] for details). In principle, excluded-volume interactions can be taken into account through the exponent c [14,15], which will essentially determine the nature of denaturation transitions (see below).

The model is most easily formulated within the grand canonical ensemble, where the total chain length L is allowed to fluctuate. In this section, we closely follow the grand canonical approach adopted in Refs. [14,15]. First, note that the explicit form of the grand partition function depends on "boundary conditions." References [14,15] adopt the boundary condition that two monomers at one end of the molecule are assumed to be bound [14,15]. On the other hand, two monomers at the other end are assumed to be either bound [14] or free (unbound) [15]. In the thermodynamic limit (which we shall focus on later), the boundary becomes minimal. Following Ref. [15], the grand canonical partition function, $\mathcal{Z}$, is given by

$$\mathcal{Z}(z) = \sum_{L=0}^{\infty} Z(L) z^L = \frac{V_0(z)Q(z)}{1-U(z)V(z)}, \tag{1}$$

where $Z(L)$ is the canonical partition function for chain length L, z is the fugacity, and

$$U(z) = \sum_{\ell=1}^{\infty} \Omega(2\ell) z^{\ell} = \sum_{\ell=1}^{\infty} \frac{s^{\ell}}{\ell^{c}} z^{\ell},$$

$$V(z) = \sum_{\ell=1}^{\infty} w^{\ell} z^{\ell}. \tag{2}$$

Finally, $V_0(z)=1+V(z)$ is the grand partition function of the bound end and $Q(z)$ is the grand partition function of the denaturated end segment [15]. (Below the denaturation temperature, the explicit form of this term is not required [15].)

To set the average chain length, one has to choose a fugacity such that $\langle L\rangle = \partial \ln \mathcal{Z} / \partial \ln z$. The fraction of bound monomer pairs θ is experimentally measurable and is chosen to be the order parameter of the transition. In this formalism, the average number of bound pairs in a chain is given by $\langle m\rangle = \partial \ln \mathcal{Z} / \partial \ln w$ [13–15], so that

$$\theta = \lim_{L\to\infty} \frac{\langle m\rangle}{\langle L\rangle} = -\frac{\partial \ln z^{*}}{\partial \ln w}. \tag{3}$$

Here, z^{*} is the value of the fugacity in the thermodynamic limit $\langle L\rangle \to \infty$: $U(z^{*})V(z^{*})=1$. (The negative sign in the second term, which is missing in Refs. [14,15], is to ensure $\theta \geqslant 0$—see Eq. 3.18 in Ref. [13].)

The nature of the denaturation transition is determined by the temperature dependence of the fugacity $z^{*}(w)$ [14,15]. Depending on the value of the exponent c, we can expect three distinct possibilities: (i) For $c \leqslant 1$, no denaturation occurs—two strands are always bound. (ii) For $1 < c \leqslant 2$, thermal denaturation is a continuous transition, while (iii) for $c > 2$ it is a first-order phase transition.

When the effect of excluded volume is suppressed, $c = d/2$. As a result, denaturation is a continuous transition for $2 < d \leqslant 4$ and a first-order phase transition for $d > 4$, but there is no transition for $d \leqslant 2$. In a more realistic case, the excluded volume interaction modifies the exponent to $c = 3/2$ for $d=2$ and $c \approx 1.766$ for $d=3$. (Note that $c \simeq 1.75$ used in Ref. [16] is somewhat smaller than this.) Thus the transition is sharper, but still continuous, in three dimensions [14–16]. More recently, it was shown [14,15] that the excluded volume interactions between denaturated loops and the rest of the chain make the phase transition first order for $d \geqslant 2$. Reference [21] also reached the conclusion that excluded volume makes the transition first order, by creating a repulsive barrier to base pairing.

B. Generalized Model: stacking vs base pairing

A natural extension of the approach introduced in Sec. II A is to allow stacking in both bound parts and loops. Stacking between monomers in bound parts can be considered as renormalizing the binding energy E_0: $E_0 \to E = E_0 + 2E_s$, where E_s is the stacking energy between two consecutive bases along the same strand. (Notice that the factor 2 is to reflect the fact that stacking occurs between stacking pairs in two strands.) On the other hand, stacking in the loop parts is nontrivial to incorporate. Nevertheless, we can still use the general form of Eq. (1)—stacking in the loop parts will alter

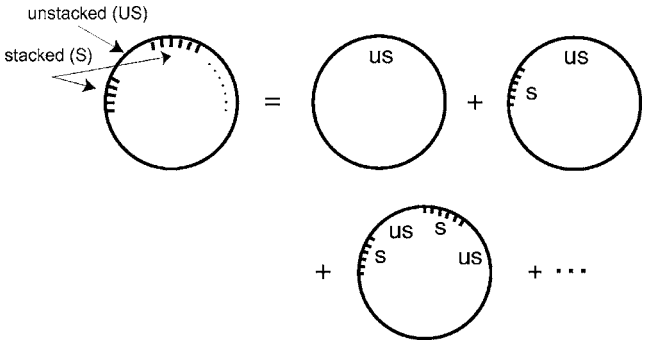

FIG. 2. Diagrammatic expansion of the partition function of loops $U(k)$ used to obtain Eq. (10). The diagram on the left hand side illustrates a loop consisting of stacked (s) and unstacked (us) bases. Stacking interactions tend to align two consecutive bases with each other in parallel, while the chain entropy prefers random (unstacked) conformations. The first diagram on the right hand side corresponds to $U_{us}(k)$ and the rest can be summed up to yield $[U_{us}(z,k)U_{s}(z,k)]/[1-U_{us}(z,k)U_{s}(z,k)]$.

$U(z)$: $U(z) \to U(z,E_s)$, which has yet to be determined. As a result, the grand canonical partition function of our stacking chain, $\Gamma(z)$, is given by

$$\Gamma(z) = \frac{V_0(z,E)Q(z,E_s)}{1 - U(z,E_s)V(z,E)}. \tag{4}$$

Here, the function $V(z,E)$ is the same as in Sec. II A with E_0 replaced by E, i.e.,

$$V(z,E) = \sum_{\ell=1}^{\infty} e^{-\ell E/k_B T} z^{\ell}, \tag{5}$$

and thus $V_0(z,E)=1+V(z,E)$. Finally, $Q(z,E_s)$ describes the denaturated end (the explicit form of this term is not needed here).

To further proceed with the result in Eq. (4), we need to explicitly calculate $U(z,E_s)$, the grand partition function of a loop. To this end, we first consider a loop consisting of stacked and unstacked bases, as schematically shown in Fig. 1 (also see Fig. 2). The canonical partition function of a loop of length ℓ (in units of the monomer size) is given as the sum over all realizations of loop conformations, which are characterized by the angles: θ_n and ϕ_n, where θ_n (ϕ_n) is the polar (azimuthal) angle of base $n+1$ with respect to base n. Here, we use a simple model of stacking [28,29]: If and only if two consecutive bases (on the same strand) are aligned in parallel or stacked, they gain an energy E_s (<0). Otherwise, they are free to bend or rotate around each other like a freely jointed chain. This amounts to assuming that two consecutive bases interact with each other through a short-range, ϕ_n-independent potential of the form: $E_s \delta(\cos\theta_n - 1)$. As a result, the Hamiltonian of the loop is simply $\mathcal{H} = E_s \Sigma_{n=1}^{\ell} \delta(\cos\theta_n - 1)$. As it turns out, the corresponding statistical weight is given by

$$\mathcal{W}[\theta_n] \equiv e^{-\beta\mathcal{H}} = \prod_{n=1}^{\ell} [1 + \omega(e^{\beta E_s} - 1)\delta(\cos\theta_n - 1)], \quad (6)$$

where ω is a phenomenological parameter that accounts for entropy changes involved in stacking [29] (see also endnote [31]). Throughout this paper, $\beta = 1/k_B T$. For simplicity, we take $\omega = 1$.

The canonical partition function of a loop of contour length ℓ, denoted by $Z_{\text{loop}}(\ell)$, can be written as

$$Z_{\text{loop}}(\ell) = \int \mathcal{D}[\Omega_n]\delta\left(\int_0^{\ell} \vec{u}_n dn\right) e^{-\beta\mathcal{H}}, \quad (7)$$

where $\mathcal{D}[\Omega_n] = \Pi_{n=1}^{\ell} d\Omega_n$, $d\Omega_n = (d\cos\theta_n)d\phi_n$, and $\vec{u}_n$ is the unit vector tangent to monomer n. The grand partition function then becomes

$$U(z, E_s) = \sum_{\ell=1}^{\infty} Z_{\text{loop}}(\ell) z^{\ell} = \int \frac{d^3k}{(2\pi)^3} U(z,k), \quad (8)$$

where

$$U(z,k) = \sum_{\ell=1}^{\infty} z^{\ell} \int \mathcal{D}[\Omega_n] e^{i\vec{k}\cdot\int_0^{\ell}\vec{u}_n dn - \beta\mathcal{H}} \quad (9)$$

is the grand partition function of a system interacting with an imaginary field $-i\vec{k}\cdot\vec{u}_n/\beta$.

With the same spirit as in the derivation of $\mathcal{Z}(z)$ in Eq. (1), using a diagrammatic expansion in Fig. 2, we find

$$U(z,k) = U_{\text{us}}(z,k) + \frac{U_{\text{us}}(z,k)U_{\text{s}}(z,k)}{1 - U_{\text{us}}(z,k)U_{\text{s}}(z,k)}, \quad (10)$$

where U_{us} and U_{s} are, respectively, the grand partition functions of unstacked and stacked parts (in the imaginary field $-i\vec{k}\cdot\vec{u}_n/\beta$). Note that the structure of this looks somewhat different from that of $\mathcal{Z}$ in Eq. (1). This is not surprising, since the topology is different for the two cases [also see Appendix A, in which open and closed (i.e., loops) chains are contrasted]. Except in the first diagram, equal numbers of stacked and unstacked parts alternate in all other diagrams in Fig. 2.

To calculate the canonical partition function of a stacked part $Z_{\text{s}}(k)$, imagine adding a stack of n monomers to an already existing monomer. As a result, there will be $n+1$ monomers stacked including the previously existing one. This reasoning leads to the following free energy:

$$Z_{\text{s}}(k) = \frac{1}{4\pi}\int_0^{2\pi} d\phi \int_{-1}^{1} d(\cos\theta) e^{iknb\cos\theta}(e^{-\beta E_s} - 1)^n$$
$$= \left(\frac{\sin nkb}{nkb}\right)(e^{-\beta E_s} - 1)^n, \quad (11)$$

where θ is the angle between $\vec{k}$ and the stacked part (if θ is the polar angle of the stacked part, then $\vec{k}$ is assumed to be aligned with the z axis, *not* to be confused with the fugacity) and b is the monomer size. Notice the factor $1/4\pi$ in front of the integral, which was introduced to ensure that the combined system (the previously existing monomer and those stacked with it) gains stacking energy E_s only, not entropy. Thus, the grand partition function of the stacked part becomes

$$U_{\text{s}}(z,k) = \sum_{n=1}^{\infty} \left(\frac{\sin nkb}{nkb}\right)(e^{-\beta E_s} - 1)^n z^n. \quad (12)$$

For an unstacked part (for one monomer), we find

$$Z_{\text{us}}(k) = \int_0^{2\pi} d\phi \int_{-1}^{1} d(\cos\theta) e^{ikb\cos\theta} = 4\pi\left(\frac{\sin kb}{kb}\right), \quad (13)$$

where θ is the angle between $\vec{k}$ and the monomer. The grand partition function for the unstacked part is then

$$U_{\text{us}}(z,k) = \sum_{n=1}^{\infty} (4\pi)^n \left(\frac{\sin kb}{kb}\right)^n z^n. \quad (14)$$

Strictly speaking, the total number of monomers in a loop must be even—each diagram in Fig. 2 is subject to this constraint. Except for the first diagram on the right hand side, it is formidable, if not impossible, to incorporate this, since the sums in Eqs. (12) and (14) cannot be performed independently. On the other hand, for large n, this becomes irrelevant. Here and in what follows, we ignore this complication and assume that n is a positive integer. Note that this is a reasonable assumption near T_c.

To summarize, the grand canonical partition function (for simplicity, we set $b = 1$), after summing up the series, is given by [32]

$$\Gamma(z) = \frac{V_0(z,E)Q(z,E_s)}{1 - U(z,E_s)V(z,E)}. \quad (15)$$

Here

$$V(z,E) = -\frac{\tilde{w}z}{\tilde{w}z - 1},$$

$$U(z,E_s) = \int \frac{d^3k}{(2\pi)^3}\left[U_{\text{us}}(z,k) + \frac{U_{\text{us}}(z,k)U_{\text{s}}(z,k)}{1 - U_{\text{us}}(z,k)U_{\text{s}}(z,k)}\right],$$

$$U_{\text{s}}(z,k) = \frac{-1}{2k}\tan^{-1}\left[\frac{2\bar{z}(-1 + \bar{z}\cos k)\sin k}{1 - 2\bar{z}\cos k + \bar{z}^2\cos 2k}\right],$$

$$U_{\text{us}}(z,k) = \frac{-4\pi z\sin k}{4\pi z\sin k - k}, \quad (16)$$

where $\tilde{w} = e^{-\beta E} = we^{-\beta E_s}$, $V_0(z,E) = 1 + V(z,E)$, and $\bar{z} = z(e^{-\beta E_s} - 1)$.

Before further proceeding with Eq. (16), it's worth considering the limit: $E_s \to 0$. In this limit, $U_{\text{s}}(z,k) = 0$ and $U(z,k) = U_{\text{us}}(z,k)$. We then have

$$U(z) = \int \frac{d^3k}{(2\pi)^3} U_{\rm us}(k) = \sum_{n=1}^{\infty} (4\pi z)^n \int \frac{d^3k}{(2\pi)^3} \left(\frac{\sin k}{k}\right)^n. \tag{17}$$

If we use $(\sin k/k)^n \approx \exp(-nk^2/6)$ (works well for large n and small k), we find

$$U(z) = \sum_{n=1}^{\infty} \frac{A(4\pi z)^n}{n^{3/2}}, \tag{18}$$

where $A=(6\pi)^{3/2}/(2\pi)^3 \approx 0.35$. In this case, our $U(z)$ reduces to that in PS model as expected. As a result, the grand partition function in Eq. (16) reduces to the one in Eq. (4).

III. RESULTS AND DISCUSSIONS

Of practical interest is the fraction of bound base pairs, which is experimentally measurable [5–9]. At sufficiently low temperatures, all bases are bound to each other, while, at too high temperatures, they are all unbound. Thus, θ decreases from one to zero as the temperature increases. As we discussed in Sec. II, the fraction of bound pairs is defined as $\theta=-\partial \ln z^*/\partial \ln w$. The thermodynamic limit $\langle L\rangle \to \infty$ is obtained by letting z approach the lowest fugacity z^* for which the partition function diverges [14,15]. This is realized for z^* satisfying

$$U(z^*) = \frac{1}{V(z^*)} = \frac{1}{(wz^*)} - 1. \tag{19}$$

Taking the derivative of the first and last terms with respect to z^*, one can find

$$\theta = \frac{1}{1 + wz^{*2} \int \frac{d^3k}{(2\pi)^3} \frac{\partial U(z^*,k)}{\partial z^*}}. \tag{20}$$

Note that U does not depend on w, while V does [i.e., $V=V(z^*,w^*(z^*))$]. It is thus much easier to calculate $\partial U(z^*)/\partial z^*$ than $\partial[1/V(z^*,w(z^*))]/\partial z^*$. This explains why θ is expressed in terms of U, not V. The equation along with Eq. (16) and Eq. (19) can be used to evaluate θ.

The expression for θ in Eq. (20) enables us to study the effect of stacking on DNA stability. In a minimalist approach, one can consider stacking as renormalizing base pairing: Stacking energy E_s simply adds to base-pairing energy E_0. However, this oversimplifies the picture as evidenced below.

Using Eq. (20), we have calculated $\theta(T)$ as a function of T (in units of room temperature) and plotted our results in Fig. 3 [32]. We have chosen $E=E_0+2E_s=-3$ (in units of k_BT at room temperature) for different choices of E_s; we have suppressed potential T dependence of E_0 and E_s. Note that our choices of E and E_s should not be taken literally, since we set $\omega=1$ (ω is largely unknown) and use other approximations. For $E_s=0$, $\theta(T)$ seems to behave as $(T-T_c)^{1/2}$ close to the denaturation temperature T_c, at which $\theta=0$. This observation is inconsistent with Refs. [14–16], which support $\theta(T)\sim(T-T_c)$ near T_c for ideal chains (i.e., $E_s=0$). But notice that this result is based on a large n approximation, which amounts to taking $(\sin k/k)^n=\exp(-nk^2/6)$. When we used this approximation with $E_s=0$, we indeed confirmed the linear dependence of θ on $(T-T_c)$ (not shown in Fig. 3).

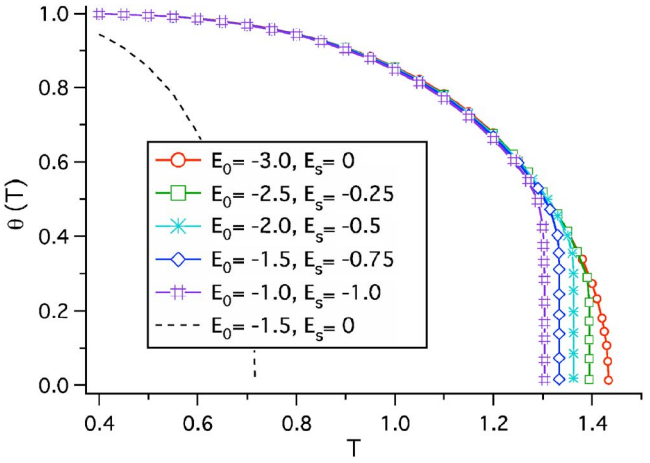

FIG. 3. (Color online) The fraction of bound monomers $\theta(T)$ as a function of temperature T for $E=-3$ (T is given in units of room temperature and E in units of k_BT at room temperature). For the three curves with symbols, the total energy $E=E_0+2E_s$ is held fixed. The denaturation transition occurs at smaller T for larger $|E_s|$. This implies that stacking in loops tends to destabilize DNA. (This is the only possible interpretation, since stacking in bound states enhances the DNA stability as does base pairing.) The most salient feature is that base stacking *sharpens* the transition—the transition becomes shaper as $|E_s|$ increases. In this analysis, we ignore potential T dependence of E_s and E_0. (To construct this figure, we have adopted a rather coarse-grained model of stacking and thus the parameters used here should not be taken literally.)

At low temperatures, there is no essential difference between the nonstacking (or $E_s=0$) and stacking cases ($E_s<0$). This is not surprising: Most of the monomers are bound and stacking can be considered as renormalizing the base-pairing energy. On the other hand, they differ at higher temperatures, especially close to T_c. This tends to invalidate a renormalized-parameter approach, in which both stacking and base pairing are subsumed into a single parameter E_0. Below we summarize the dominant features of θ near T_c ($T \lesssim T_c$).

First, for given T and E, θ decreases as $|E_s|$ increases. As a result, the denaturation temperature is lower for larger $|E_s|$. In other words, stacking in loops destabilizes dsDNA. At first glance, this is puzzling: For stronger stacking strength (and for given E), the entropic gain for loops is less significant. From an entropy consideration only, this implies that DNA is more stable for larger $|E_s|$. This reasoning is, however, erroneous. To illustrate the role of stacking, imagine changing E_s from zero to a negative value, while keeping $E=E_0+2E_s$ fixed. When $E \approx 2E_s$ and $E_0 \approx 0$, two strands become almost decoupled. The resulting system is essentially two noninteracting or weakly interacting strands, which can be relatively easily denaturated. This may explain the general trend of our results in Fig. 3. On the other hand, the overall stability is enhanced by stacking. To see this, we have compared inverted triangles ($E_0=-1.5$, $E_s=-0.75$) with the dotted line

($E_0=-1.5$, $E_s=0$); E_0 is the same for the two cases, but E_s is set to zero in the latter. The former corresponds to much higher T_c, indicating that stacking enhances the stability.

Second, stacking makes the transition sharper; it appears that the transition is first order. To further confirm this observation, we have studied the nature of the transition from a different angle. To this end, we have considered the functions $U(z,E_s)$ and $V(z,E)$ in Eq. (4) as a function of z. This consideration compliments our finding that the transition is first order for $E_s \neq 0$ (see Appendix B for details). This is illuminating, as it indicates that sharp transitions observed experimentally may be attributed to stacking interactions. On the other hand, earlier results [14,15] suggest that excluded volume interactions are required for sharp transitions (when stacking in loops is not included). It is natural to expect both stacking and the excluded-volume interaction to be responsible for the sharp transition. While our observation is analogous to the repulsive barrier proposed in Ref. [21], it is unique in the sense that long-distance (along the contour) interactions are not required. Importantly, this finding is based on an almost exactly solvable model and is not obscured by uncontrollable approximations or *ad hoc* assumptions. A plausible reason for our finding is as follows: Stacking in loops reduces the weight of the loop (or the "ring-closure" probability); in other words, it enhances the barrier to ring-closure (the free energy cost for looping is higher for larger $|E_s|$). One possible speculation is that this unfavorable free energy can be reduced if two loops merge into each other to form a bigger loop—this can create a tendency for DNA to denaturate more abruptly.

IV. CONCLUSIONS

To summarize, we have presented a theoretical formalism for describing the thermal stability of double-stranded DNA by treating base stacking and base pairing on an equal footing. The main focus has been on studying how stacking influences the nature of thermal denaturation. The effects of base stacking are nontrivial: While stacking in bound states enhances the stability as does base pairing, stacking in loops makes denaturation transitions sharp—the overall stability is enhanced by stacking. This implies that both base stacking and base pairing should be included simultaneously. Our analysis of the transition in term of the fraction of bound monomers, presented in Fig. 3, has been further augmented by the graphical analysis of $U(z)$ and $V(z)$ in Eq. (16)—see Appendix B. (While the former analysis is more experimentally accessible, the later is more analogous to those in Refs. [14,15].) The graphical analysis also shows how stacking can sharpen the transition.

Molecular details ignored in this work can easily complicate the analysis. As it turns out, different stacks (i.e., two consecutive bases along the same strand) show varying levels of stacking tendency [2,33]: Stacking is strongest for purine-purine stacks (e.g., A-A and G-G) and weakest for pyrimidine-pyrimidine stacks (e.g., T-T); purine-pyrimidine stacks (e.g., A-T) show an intermediate level of stacking. On the other hand, base pairing is stronger for G-C pairs than for A-T pairs. Consideration of both effects simultaneously is formidable, if not impossible, and goes beyond the scope of this work. In addition, we have not considered the geometric constraint imposed on loops, i.e., a "Y-fork" topology: Formation of a loop may require additional breakage of stacking at a Y-fork formed between a bound part and an adjacent loop. This extra complexity can change the stability. Finally, the chain entropy of bound parts and "mis-folding" of loops (base pairing within each loop) ignored here will also complicate the picture. Further investigation is certainly warranted.

ACKNOWLEDGMENTS

We acknowledge helpful discussions with J. Z. Y. Chen. This work was supported by NSERC (the Natural Sciences and Engineering Research Council in Canada) and CFI (the Canadian Foundation of Innovation). One of us (B.Y.H.) benefited from scientific stimulations at the focus program on biopolymers and biomembranes held in Feb. 2–12, 2004 at the APCTP (the Asian Pacific Center for Theoretical Physics, Korea).

APPENDIX A

The main difference in structure between Eqs. (1) and (10) arises from their topological difference: "open" vs "closed." It proves useful to consider a single-stranded linear (open) chain, for which one can obtain the canonical free energy (and thus the grand free energy)—we will eventually let the chain form a loop. This consideration will elucidate our diagrammatic expansion adopted in Sec. II B (see below). By mapping the linear chain onto a linear array of "two-state systems," in which two consecutive monomers are either stacked or unstacked, one can readily obtain the canonical free energy: With $w_s=e^{-\beta E_s}-1$, $Z_n=4\pi(4\pi+w_s)^{n-1}$, where n is the number of monomers. This leads to the grand free energy

$$U_o=\sum_{n=1}^{\infty}4\pi(4\pi+w_s)^{n-1}z^n=\frac{-4\pi z}{-1+(4\pi+w_s)z}, \quad \text{(A1)}$$

where the subscript "o" refers to open conformations and our notation U_o for the grand free energy was chosen in parallel with $U(z,k)$ in Eq. (10). Note that $n=0$ is excluded in the sum as in Eqs. (2), (12), and (14)—the purpose of this calculation is in part to contrast the linear case against the loop in Fig. 2.

We can also obtain the grand free energy using a diagrammatic expansion. To this end, by taking $k\to 0$ in Eqs. (12) and (14), we obtain

$$U_s^{(0)}=U_s(z,k\to 0)=\sum_{n=1}^{\infty}(w_s z)^n=\frac{-w_s z}{-1+w_s z}, \quad \text{(A2a)}$$

$$U_{us}^{(0)}=U_{us}(z,k\to 0)=\sum_{n=1}^{\infty}(4\pi z)^n=\frac{-4\pi z}{-1+4\pi z}. \quad \text{(A2b)}$$

Not surprisingly, these are identical to those for the linear case—in the limit $k\to 0$, the ring-closure condition becomes

irrelevant. The grand canonical partition function is then

$$U^{(0)} = U_{us}^{(0)} + U_{us}^{(0)}U_s^{(0)} + U_{us}^{(0)}U_s^{(0)}U_{us}^{(0)} + U_{us}^{(0)}U_s^{(0)}U_{us}^{(0)}U_s^{(0)} + \cdots = \frac{U_{us}^{(0)}(1+U_s^{(0)})}{1-U_{us}^{(0)}U_s^{(0)}}. \quad \text{(A3)}$$

Note that the series starts with unstacked (i.e., a single monomer at one end of the chain). For this reason, we do not include $U_s^{(0)}$—single monomers cannot be stacked. If combined with the results in Eq. (A2), Eq. (A3) reduces to U_o as expected.

Now imagine the chain forming a loop. Obviously nonzero-k contributions should come into play. This does not mean that we can simply turn on k dependence in the diagrammatic expansion in Eq. (A3). One should note that not all terms in Eq. (A3) are unique when they represent a loop. For example, $U_{us}U_sU_{us}$ is not distinct from $U_{us}U_s$ and is thus redundant. Obviously one should include the latter. Except for U_{us}, only even-power terms will survive [see Eq. (10) and Fig. 2].

APPENDIX B

This appendix will elucidate our picture of base stacking as sharpening the denaturation transition. Our discussion is based on Refs. [14,15] but requires a nontrivial generalization to include stacking. As in Sec. II B, we will largely ignore excluded volume. As discussed in Refs. [14,15] for the nonstacking case $E_s=0$, the existence and nature of denaturation transitions are mainly determined by the behavior of $U(z)$ near $z=1/s$ (we set $s=4\pi$), which depends on loop statistics (e.g., the exponent c). (Note that, for given energy E, V depends on T and z only.)

First, recall that $\theta=[1+wz^{*2}\alpha]^{-1}$, where $\alpha \equiv \partial U(z^*)/\partial z^*$. Graphically z^* can be obtained by locating z at which $U(z)$ crosses $1/V(z)$: $U(z^*)=1/V(z^*)=1/wz^*-1$. A few graphs of U and $1/V$ are shown in Fig. 4 (see the caption for details); U $(1/V)$ is a monotonically increasing (decreasing) function of z and thus there is only one z^* for given E_s and T. Also note that there exists a special value of z (to be denoted by z_∞) beyond which $U(z)$ diverges, as described by the gray vertical lines in Fig. 4 [this can readily be seen from Eq. (2) for $E_s=0$]. As it turns out, for $E_s\neq 0$, z_∞ is the zero of $[1-U_{us}(z,k)U_s(z,k)]_{k\to 0}$ [see Eq. (10) or Eq. (16)]—there is only one zero. On the other hand, for $E_s=0$, $z_\infty=1/4\pi$ is the zero of $4\pi z \sin k-k$, the denominator of U_{us} in Eq. (16), in the limit $k\to 0$. As T increases, the curve $1/V(z)$ shifts to the right and thus z^* increases; it approaches the curve $z^{-1}-1$ as $T\to\infty$. This sets the maximum value of z^* denoted by z_M^* corresponding to $T\to\infty$: $U(z_M^*)=1/z_M^*-1$. Depending upon the values of z_∞ and z_M^*, there can arise a few distinct possibilities:

(1) $z_M^*<z_\infty$: In this case, z^* increases monotonically as T increases. On the other hand, $U(z^*)$ remains finite for $z \leqslant z_M^*$. As a result, $\alpha \equiv \partial U(z^*)/\partial z^*$ is always finite. This means that $\theta>0$ for any T and thus there is no transition. This can be realized when $c\leqslant 1$ and $E_s=0$ [14,15] (not shown in Fig. 4). As discussed in the literature (see Refs. [14,15] and references therein), for ideal chains (i.e., with excluded volume "turned off"), $c=d/2$, where d is the dimensionality—there is no transition for $d\leqslant 2$.

(2) $z_M^*=z_\infty$ [this ensures $1/V(z_\infty)\geqslant U(z_\infty)$]. In this case, one can find $T=T_c$ at which $1/V(z_M^*)=U(z_M^*)$. As $T\to T_c$ from below, $z^*\to z_M^*$; beyond T_c, however, z^* remains unchanged. As a result, $\alpha\to\infty$ (thus $\theta=0$) for $T>T_c$. Depending upon the behavior of $U(z)$ around z_M^*, this case can be further classified into two subclasses: (a) If $[\partial U/\partial z]_{z\to z_M^*}\to\infty$, α decays to zero continuously as T approaches T_c, indicating a continuous transition. This can be realized for $1<c\leqslant 2$ (and $E_s=0$) as evidenced by the bottom solid curve (also see Fig. 4 in Ref. [15]). (b) If $[\partial U/\partial z]_{z\to z_M^*}<\infty$, then $\alpha<\infty$ for $T<T_c$, implying that θ changes abruptly from a finite value (>0) to zero at T_c (recall $\theta=0$ for $T\geqslant T_c$). Thus the transition is first order. For $E_s=0$, this can happen for $c>2$ (not shown in the figure), which requires excluded volume [14,15]). On the other hand, when stacking is included (i.e., $E_s\neq 0$), the transition can be first order, as indicated by the curve for $E_s=-1.0$ and $T=T_c\approx 1.3$ (in units of room temperature) in Fig. 4. This confirms the sharpness of the transition indicated in Fig. 3.

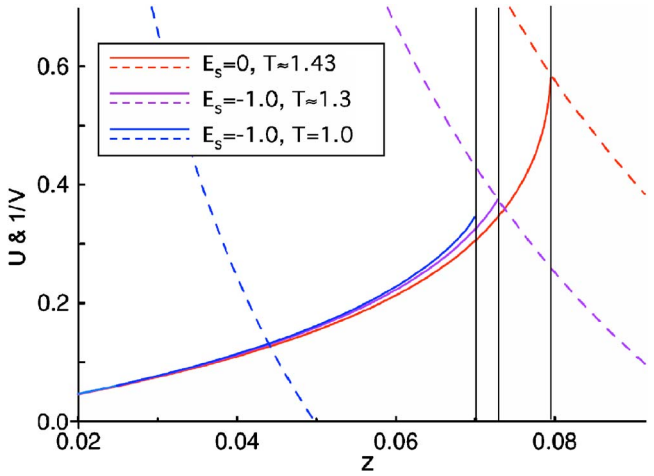

FIG. 4. (Color online) Graphs of $U(z,E_s)$ and $1/V(z,E)$ for $E=-3.0$ (in units of k_BT at room temperature). The solid lines are $U(z,E_s)$; from the bottom one, they correspond to $E_s=0$ $(T=T_c\approx 1.43)$, $E_s=-1.0$ $(T=T_c\approx 1.3)$, and $E_s=-1.0$ $(T=1.0)$, respectively (T is given in units of room temperature). The dashed lines are $1/V(z,E)$, from the one on the right, they correspond to $E_s=0$ $(T=T_c\approx 1.43)$, $E_s=-1.0$ $(T=T_c\approx 1.3)$, and $E_s=-1.0$ $(T=1.0)$, respectively. In the electronic version, different choices of the parameters are described by different colors (see the legend).

[1] B. Alberts, A. Johnson, J. Lewis, M. Raff, K. Roberts, and P. Walter, *Molecular Biology of the Cell*, 4th ed. (Garland Science, New York, 2002).
[2] G. G. Hammes, *Thermodynamics and Kinetics for the Biological Sciences* (Wiley-Interscience, Hoboken, NJ, 2000).
[3] See, for example, W. M. Gelbart, R. F. Bruinsma, P. A. Pincus, and V. A. Parsegian, Phys. Today **53**, 38 (2000).
[4] See C. Bustamante, Z. Bryant, and S. B. Smith, Nature (London) **421**, 423 (2003), and references therein.
[5] V. M. Pavlov, J. L. Lyubchenko, A. S. Borovik, and Y. Lazurkin, Nucleic Acids Res. **4**, 4053 (1977).
[6] A. S. Borovik, Y. A. Kalambet, Y. L. Lyubchenko, V. T. Shitov, and E. Golovanov, Nucleic Acids Res. **8**, 4165 (1980).
[7] R. M. Wartell and A. S. Benight, Phys. Rep. **126**, 67 (1985).
[8] O. Gotoh, Adv. Biophys. **16**, 1 (1983).
[9] M. Peyrard, Nonlinearity **17**, R1 (2004).
[10] N. Theodorakopoulos, T. Dauxois, and M. Peyrard, Phys. Rev. Lett. **85**, 6 (2000).
[11] D. Poland and H. A. Scheraga, J. Chem. Phys. **45**, 1456 (1966); J. Chem. Phys. **45**, 1464 (1966).
[12] D. Poland and H. A. Scheraga, *Theory of Helix-Coil Transitions in Biopolymers* (Academic, New York, 1970).
[13] F. W. Wiegel, in *Phase Transitions and Critical Phenomena*, edited by C. Domb and J. L. Lebowitz (Academic, New York, 1983), Vol. 7.
[14] Y. Kafri, D. Mukamel, and L. Peliti, Phys. Rev. Lett. **85**, 4988 (2000). See also, A. Hanke and R. Metzler, Phys. Rev. Lett. **90**, 159801 (2003); Y. Kafri, D. Mukamel, and L. Peliti, Phys. Rev. Lett. **90**, 159802 (2003).
[15] Y. Kafri, D. Mukamel, and L. Peliti, Eur. Phys. J. B **27**, 135 (2002).
[16] M. E. Fisher, J. Chem. Phys. **45**, 1469 (1966).
[17] D. K. Lubensky and D. R. Nelson, Phys. Rev. E **65**, 031917 (2002).
[18] D. Cule and T. Hwa, Phys. Rev. Lett. **79**, 2375 (1997); L. H. Tang and H. Chate, Phys. Rev. Lett. **86**, 830 (2001).
[19] S. Cocco and R. Monasson, Phys. Rev. Lett. **83**, 5178 (1999).
[20] M. Barbi, S. Lepri, M. Peyrard, and N. Theodorakopoulos, Phys. Rev. E **68**, 061909 (2003).
[21] T. Garel, C. Monthus, and H. Orland, Europhys. Lett. **55**, 132 (2001).
[22] W. Sung and J. H. Jeon, Phys. Rev. E **69**, 031902 (2004).
[23] D. K. Lubensky and D. R. Nelson, Phys. Rev. Lett. **85**, 1572 (2000).
[24] J. Z. Y. Chen, Phys. Rev. E **66**, 031912 (2002).
[25] B. Tinland, A. Pluen, J. Sturm, and G. Weill, Macromolecules **30**, 5763 (1997).
[26] S. B. Smith, Y. Cui, and C. Bustamante, Science **271**, 795 (1996).
[27] J. B. Mills, E. Vacano, and P. J. Hagerman, J. Mol. Biol. **285**, 245 (1999).
[28] A. Sain, B.-Y. Ha, H.-K. Tsao, and J. Z. Y. Chen, Phys. Rev. E **69**, 061913 (2004).
[29] A. Sain, J. Z. Y. Chen, and B.-Y. Ha (unpublished).
[30] M. Doi and S. F. Edwards, *The Theory of Polymer Dynamics* (Oxford University Press, Oxford, 1986).
[31] Notice the combination $(e^{-\beta E_s}-1)$—this is to ensure that the stacking chain becomes a freely-jointed chain in the limit $E_s \to 0$. In a more elaborated approach [28], $\omega(e^{-\beta E_s}-1)$ was used in place of $(e^{-\beta E_s}-1)$, where ω describes the entropic loss for two stacked bases, which are not allowed to rotate about their own axis, i.e., "spin." For simplicity, here we choose $\omega=1$.
[32] Note that $U_{\rm us}(z,k)$ in Eq. (16) includes $n=1$ term [see Eq. (14)]. However, this term should not contribute to $U_{\rm us}$, since a single monomer cannot make a loop. Indeed, $\int d^3k/(2\pi)^3 \times(\sin kb/kb)=\delta^3(b)$, which is zero for $b\neq 0$. In our numerical calculations, we cut off large k contributions $(k>\pi/b=\pi)$ and thus this integral does not become a delta function. Nevertheless, we observe that the contribution of $n=1$ term is still small and will not change Fig. 3 noticeably.
[33] C. R. Cantor and P. R. Schimmel, *Biophysical Chemistry* (W.H. Freeman, New York, 1980).